ELSEVIER

Journal of Molecular Catalysis A: Chemical 145 (1999) 183–201

JOURNAL OF MOLECULAR CATALYSIS A: CHEMICAL

www.elsevier.com/locate/molcata

Influence of oxychlorination treatment on the surface and bulk properties of a Pt–Sn/Al_2O_3 catalyst

Geomar J. Arteaga, James A. Anderson, Susanne M. Becker, Colin H. Rochester *

Chemistry Department, Dundee University, Dundee DD1 4HN, UK

Received 13 July 1998; accepted 19 November 1998

Abstract

A Pt(3%)–Sn(4.5%)/Al_2O_3 catalyst has been studied after treatments prior to reduction involving calcination in air at 673 K or 823 K, or oxychlorination in air + 1,2-dichloropropane at 823 K. Bulk phases present were characterised by XRD and surface character was probed by IR of adsorbed CO and by CO chemisorption. Comparative IR and chemisorption results for Pt(3%)/Al_2O_3 are also presented. Pt–Sn/Al_2O_3 was used to catalyse heptane reforming reactions. Catalyst prepared from a chlorine-free precursor and calcined at 673 K contained well-dispersed SnO_2 and PtO_2 but no Pt°, whereas calcination at 823 K gave Pt° particles covered with a layer of O-adatoms. After reduction both catalysts contained Pt° particles, the surfaces of which, although exposing arrays of Pt° atoms, were partly covered in Sn°. No alloy was formed. Tin, probably as Sn^{2+}, was also spread over the alumina support surface. The spreading of Sn over both Pt and alumina was greater after the higher temperature calcination pretreatment followed by reduction. Oxychlorination also gave Pt° particles with surface O-adatoms and probably surface Cl together with segregated crystalline SnO_2. However, in marked contrast to the Cl-free catalysts, subsequent reduction gave 1:1 PtSn alloy particles with excess Sn spread over the alumina. Alloy surfaces did not exhibit large ensembles of exposed Pt° atoms. Alloy formation reduced catalyst activity but induced stability with respect to both activity and selectivity. Both alloy formation, and coking with time for catalysts with arrays of exposed Pt, promoted isomerisation reactions, but decreased aromatisation, hydrogenolysis and C_5 cyclisation. Selectivity changes accompanying alloy formation are discussed and the results are primarily attributed to geometric ensemble effects.

Keywords: CO adsorption on Pt–Sn; Pt–Sn/Al_2O_3 reforming catalyst

1. Introduction

The addition of tin to supported Pt catalysts has a significant effect on catalytic behaviour [1–3] and therefore the role of the tin has attracted much attention [4–11]. Tin interacts strongly with the alumina support and if present as Sn(II) [1,4,6–8] weakens and reduces the number of acid sites on alumina and also eliminates basic sites [9]. Tin also enhances catalyst stability probably by suppressing coke-forming reactions [10,11] and inducing resistance to sintering. Catalyst selectivity in hexane/hydrogen reactions was altered significantly when Pt was alloyed with Sn [12,13]. In general hydrocarbon reforming reactions are carried out over alu-

* Corresponding author. Tel.: +44-1382-344327; Fax: +44-1382-345517

1381-1169/99/$ - see front matter
PII: S1381-1169(99)00092-8

mina-supported catalysts for which the presence of chlorine is an important aid to improving platinum dispersion [14,15], and this in turn influences catalyst activity and selectivity [16]. The present work was therefore designed to assess the existence of alloyed particles in a $Pt–Sn/Al_2O_3$ catalyst with and without added chlorine, to explore the surface character of the Pt component by CO uptake measurements and infrared study of CO adsorption, and to determine how changes in the bulk or surface character of the Pt influenced activities and selectivities for the reforming of heptane.

2. Experimental

Catalyst precursor was prepared by drying (evaporation to dryness at 333 K, followed by heating in air at 383 K for 15 h and then at 673 K in dry CO_2-free air for 1 h) a dispersion of Degussa non porous γ-alumina (surface area 110 $m^2\ g^{-1}$) in an aqueous solution containing tetraammineplatinum(II) hydroxide and tin(II) oxalate. Catalyst precursor, as loose powder for the X-ray diffraction (XRD), CO chemisorption and catalytic experiments and as pressed self-supporting discs for infrared examination, was subjected to a sequence of treatments involving calcination (heated at 15 K min^{-1} to 673 K and held at 673 K for 30 min in a flow of air), reduction (1 h at 673 K in flowing hydrogen), oxidation (1 h at 823 K in flowing air), reduction (as for the initial reduction), oxychlorination (1 h at 823 K in a 60 ml min^{-1} flow of air containing 510 μmol h^{-1} 1,2-dichloropropane per 50 mg catalyst), and reduction (as for the initial reduction). After reduction catalysts contained 3.0 wt.% Pt and 4.5 wt.% Sn giving a Sn/Pt molar ratio of 2.47/1.

Catalysts were studied at the various stages of the treatment sequence, either in sequential experiments involving a single sample, or in experiments involving samples which were discarded after a single characterisation or catalytic testing. Details are given in Section 3 where necessary. Transmission infrared spectra of discs at ca. 293 K were recorded using a Perkin Elmer 1710 FTIR spectrometer operating at 4 cm^{-1} resolution. Pulse chemisorption of CO at ca. 293 K was monitored with a Perkin Elmer AutoSystem XL gas chromatograph. Powder XRD patterns were recorded using CuK_α radiation at 1° 2θ min^{-1}. A Perkin Elmer 8410 gas chromatograph was used to analyse the products from heptane/hydrogen reactions over 50 mg catalyst under the following conditions: temperature 623 K; pressure 1 atm; (H_2/C_7H_{16}) molar ratio (10/1); 25 ml min^{-1} hydrogen flow; LHSV 18.2 ml heptane (g cat)$^{-1}$ h^{-1}.

3. Results

3.1. Powder XRD

Fig. 1 shows the XRD results after six stages of catalyst treatment. The pattern for catalyst calcined at 673 K was entirely attributable to the Al_2O_3 support except for broad peaks at 2θ of ca. 26.5, 34 (adding to a peak due to alumina) and 51.5° which correspond to the pattern for SnO_2. The broadness of the peaks suggests that the size of the SnO_2 crystallites was very small and hence that the Sn component of the catalyst was well dispersed over the alumina surface. There were no peaks attributable to Pt° or PtO_2. The SnO_2 peaks were greatly reduced in intensity on subsequent heating in hydrogen at 673 K in accordance with the expected reduction to SnO [9]. The absence of peaks due to SnO showed the absence of discrete crystallites, and pointed to a highly dispersed Sn(II) species. Two narrow maxima due to Pt° appeared after reduction.

The sharp maxima due to Pt° were also present although slightly broader after calcined/reduced catalyst was heated in air at 823 K. There was no evidence for SnO, SnO_2 or PtO_2. Subsequent reduction at 673 K had little effect on the

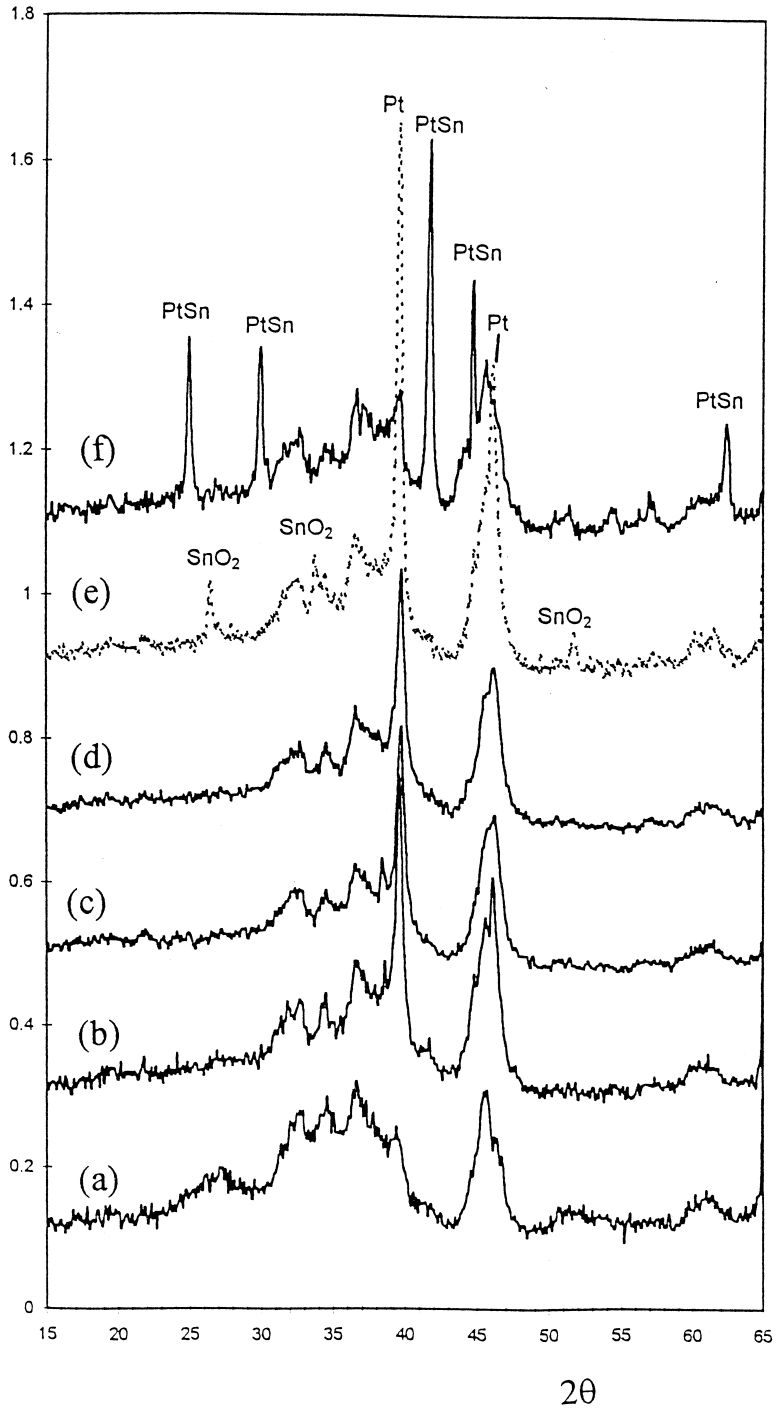

Fig. 1. XRD patterns after catalyst precursor was (a) calcined, (b) calcined/reduced, (c) calcined/reduced/oxidised, (d) calcined/reduced/oxidised/reduced, (e) calcined/reduced/oxychlorinated, and (f) calcined/reduced/oxychlorinated/reduced.

XRD pattern other than to slightly enhance the peaks due to Pt°. Thus high temperature oxidation had led to a high proportion of the Pt being present as Pt°and not PtO_2, whereas in contrast

calcination in air at 673 K failed to generate Pt° which was only formed after subsequent reduction.

XRD results for oxychlorination followed by reduction were dramatically different from those for oxidation followed by reduction. Oxychlorination gave peaks due to SnO_2 crystallites, and strong narrow peaks due to Pt°. The platinum and tin were at least in part segregated, tin in an oxidised form and platinum in a reduced form. Subsequent reduction caused the disappearance of SnO_2, the nearly complete disappearance of Pt° (a peak coincident with the Pt peak at ca. 39.5° was primarily due to alumina), and the appearance of the characteristic pattern of an hexagonal 1:1 Pt–Sn alloy [8,12,13,17]. The presence of chlorine in the oxidative treatment of Pt–Sn/Al_2O_3 catalyst precursors clearly favoured Pt–Sn alloy formation which did not occur in the absence of chlorine. Lieske and Völter [8] also found that chlorine favoured alloying of tin with platinum.

A pressed catalyst disc in the infrared cell was subjected to the treatment sequence calcination (673 K)/reduction (673 K)/oxychlorination (823 K)/reduction (673 K)/oxychlorination (823 K)/reduction (673 K) and then submitted for XRD analysis. The pattern was closely similar to that in Fig. 1f showing that catalysts treated as a loose powder and as a pressed disc gave the same results. An extra oxychlorination cycle for the pressed disc would not be expected to affect the catalyst character to a significant extent [15].

Catalyst which had been used in the reforming reaction of heptane after calcination/reduction gave the same XRD pattern as in Fig. 1b. A catalyst subjected to the consecutive series of treatments calcination/reduction/heptane reforming/oxidation/reduction/heptane reforming/oxychlorination/reduction/heptane reforming gave the same XRD pattern as in Fig. 1f. Use of catalyst for the heptane reaction at 623 K or subsequent treatment of catalyst used in a reaction had no effect on the bulk structure of Pt or Pt–Sn crystallites.

3.2. CO adsorption

Fig. 2 shows CO/Pt ratios for three catalysts for which reduction followed calcination, oxidation and oxychlorination in accordance with the XRD results in Fig. 1b, d and f, respectively. The ratios were small suggesting that exposed Pt atoms were in the surface of large particles, or that smaller particles had surfaces which were largely covered by Sn. In the absence of chlorine, raising the oxidation temperature to 823 K would reduce the dispersion for Pt alone [14] and the same result was observed here for Pt–Sn. Oxychlorination followed by reduction also decreased the Pt dispersion for Pt–Sn/Al_2O_3 showing that alloying of Pt with Sn (Fig. 1f) led to an appreciable decrease in the availability of Pt atoms in the catalyst surface. The dominant Pt° peak in the XRD pattern in Fig. 1e was more intense and had a narrower half-peak width than the Pt° peak in Fig. 1c suggesting that the Pt° crystallites were bigger after oxychlorination than after oxidation. This is not consistent with results for 0.3% Pt/Al_2O_3 [14,15] for which oxychlorination favours movement of Pt species over the alumina surface and a better Pt dispersion after reduction. For Pt–Sn the spreading of oxidic Sn species over alumina must hinder the spreading of platinum oxides or oxychlorides [15] and therefore the Pt forms bigger crystallites and hence proba-

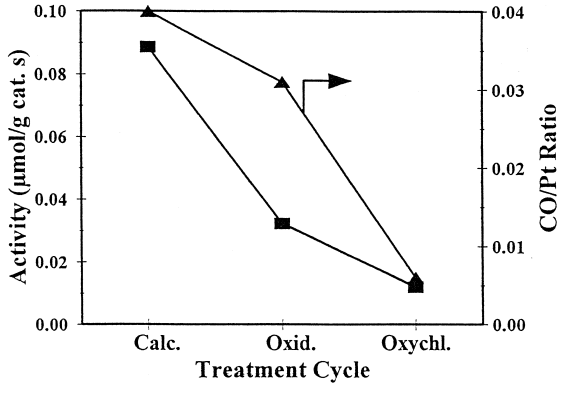

Fig. 2. CO uptakes and catalyst activities (after 0.08 h on line) for reduced Pt–Sn/Al_2O_3 after calcination, oxidation and oxychlorination pretreatments.

bly bigger particles. The subsequent agglomeration of Pt and Sn during reduction to form alloy may have retained the greater particle size and this would be partially responsible for the decreased CO/Pt ratio after oxychlorination and reduction. However, a further contributing factor to the contrast between the results for the oxidised/reduced and oxychlorinated/reduced catalysts must have been surface enrichment of Sn in Pt–Sn alloy particles [18,19].

Calcined catalyst exposed to CO gave a dominant infrared band at 2118 cm^{-1} (Fig. 3A) which resembles a band at 2120 cm^{-1} for CO on PtO_2 [20]. A weaker band at 2168 cm^{-1} is more typical of carbonyls of Pt(II) [21]. A shoulder at 2200 cm^{-1} for high CO pressures disappeared on evacuation at 293 K and was due to CO ligated to Al^{3+} sites on alumina [22]. The band did not appear for reduced catalysts perhaps partly because heat treatment in hydrogen weakens surface Lewis acidity, but mainly because Sn(II) decreases the number of acidic sites on alumina [9].

There were no oxidised Pt^{n+} species available for CO ligation in calcined/reduced catalyst. With increasing CO pressure a band initially at 2048 cm^{-1} shifted towards 2051 cm^{-1} at high coverage, but moved to 2050 cm^{-1} after evacuation (Fig. 3B). This band which is due to Pt°–CO is at a lower position than for CO on either low-index or high-index single crystal Pt surfaces [23,24], although low-wavenumber

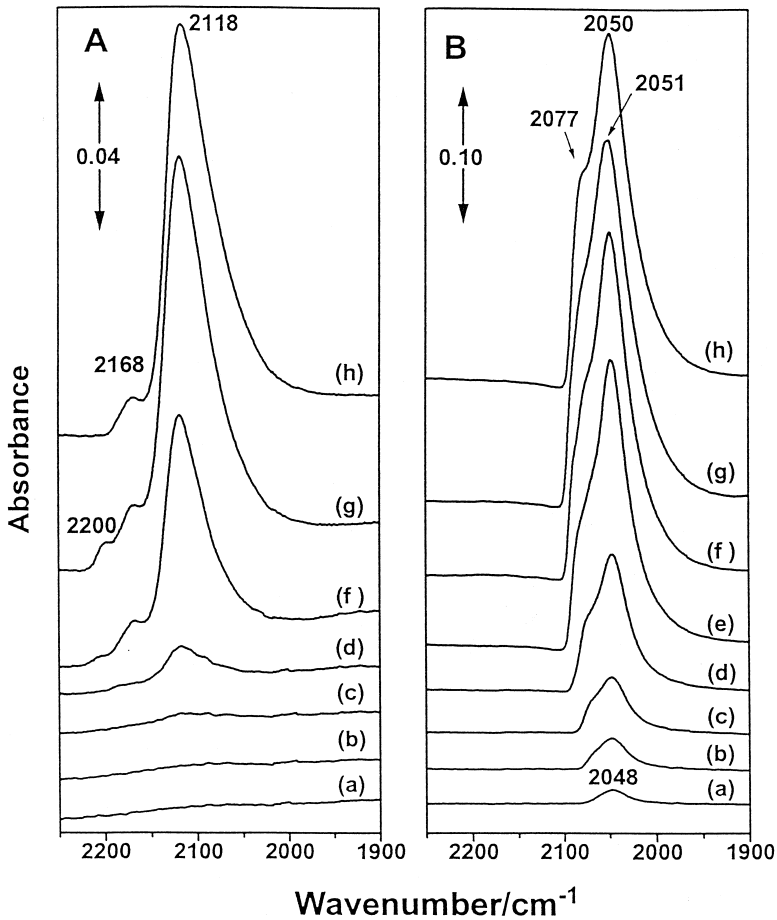

Fig. 3. Spectra of (A) calcined and (B) calcined/reduced Pt–Sn/Al_2O_3 with CO at (a) 0.05, (b) 0.08, (c) 0.11, (d) 0.27, (e) 0.53, (f) 133 and (g) 6670 N m^{-2}, and (h) after evacuation.

bands occur for evaporated Pt films [25]. Improving supported platinum dispersion tends to favour lower wavenumber ν_{CO} bands [26] which are often attributed to low coordination, high energy sites possibly at steps, kinks or edges in surfaces which do not contain extended planar arrays of Pt atoms. However, the present catalyst was apparently not highly dispersed (Fig. 2) and contained sufficiently large crystallites to generate a clear XRD pattern for Pt°. One explanation of the combined XRD, CO/Pt and IR data would be that the catalyst contained large Pt° particles (ca. 10 nm) with highly stepped or rough surfaces. However, a more likely alternative is that smaller particles of Pt° were largely covered in Sn. The dilution of exposed Pt sites by the Sn adlayer would lead to greatly reduced dipolar coupling between adsorbed CO molecules and hence a lower band position for the ν_{CO} vibration than for CO on unmodified Pt surfaces [27]. For the calcined/reduced catalyst in the absence of chlorine, therefore, both metals existed on particle surfaces but this was not accompanied by alloying in the bulk phase. A shoulder in spectra at 2077 cm^{-1} (Fig. 3B) is more consistent with CO adsorbed on extended arrays of Pt° atoms [23,24]. There was no evidence for CO interacting with tin atoms or ions in the catalyst surface.

After oxidation at 823 K Pt–Sn/Al_2O_3 gave spectra which showed that the platinum had only been partially converted to PtO_2 (Fig. 4A). The intensity of a band at 2122 cm^{-1} due to CO on PtO_2 [20] was only 40% of the intensity of

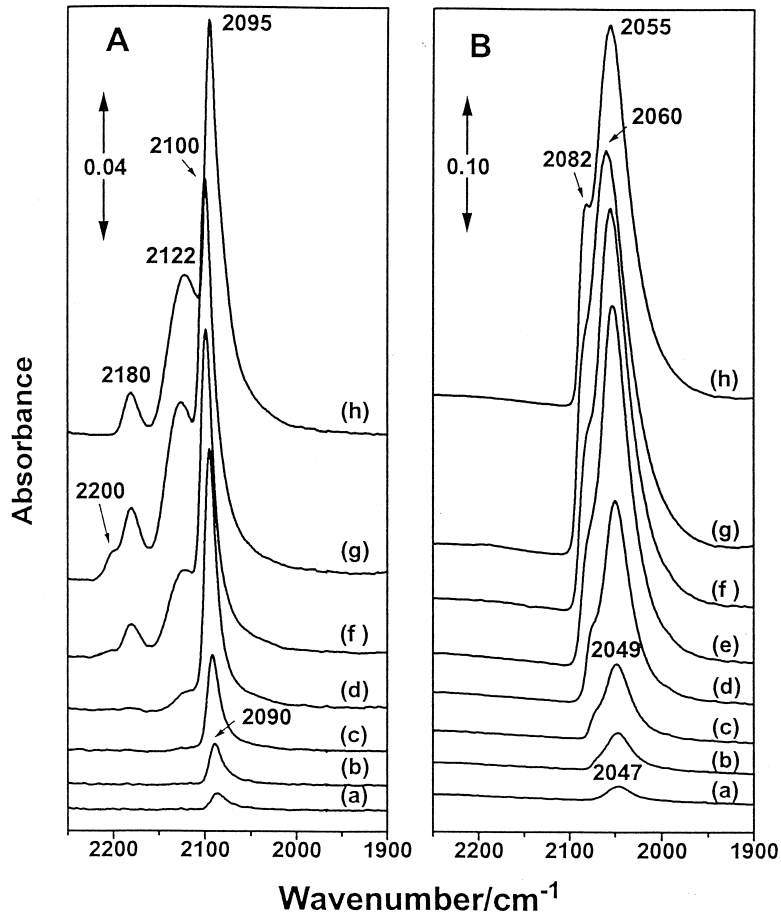

Fig. 4. Spectra as for Fig. 3 of (A) calcined/reduced/oxidised and (B) calcined/reduced/oxidised/reduced Pt–Sn/Al_2O_3.

the corresponding band after calcination at 673 K. The band associated with CO at Pt^{2+} [21] sites appeared as a separate maximum at 2180 cm^{-1} which was only slightly more intense than the shoulder at 2168 cm^{-1} for calcined catalyst. The dominant infrared band at 2100 cm^{-1} for oxidised catalyst was completely absent for calcined catalyst and may be ascribed to CO ligated to Pt sites. De La Cruz and Sheppard [24] reported a band at 2099 cm^{-1} for O-covered Pt/SiO_2 which was ascribed to adsorbed CO molecules which were influenced by the electron withdrawing effects of coadsorbed O-atoms. The XRD data showed the presence of Pt° crystallites, and the infrared spectra have shown that the surfaces of Pt° particles retained adsorbed oxygen but were not covered by a layer of oxide.

Despite the differences between the results for the calcined and oxidised catalysts subsequent reduction gave nearly identical spectra (Figs. 3B and 4B). Both the band intensities and positions were similar after the two treatments although after oxidation there was a slightly enhanced 2060 cm^{-1} band accompanied by a slightly attenuated band at 2082 cm^{-1}. This would be consistent with a greater extent of spreading of Sn over the surface of Pt° particles which would hence reduce the availability of extended arrays of Pt atoms.

The spectrum of CO on $Pt–Sn/Al_2O_3$ after an oxychlorination step (Fig. 5A) contained the

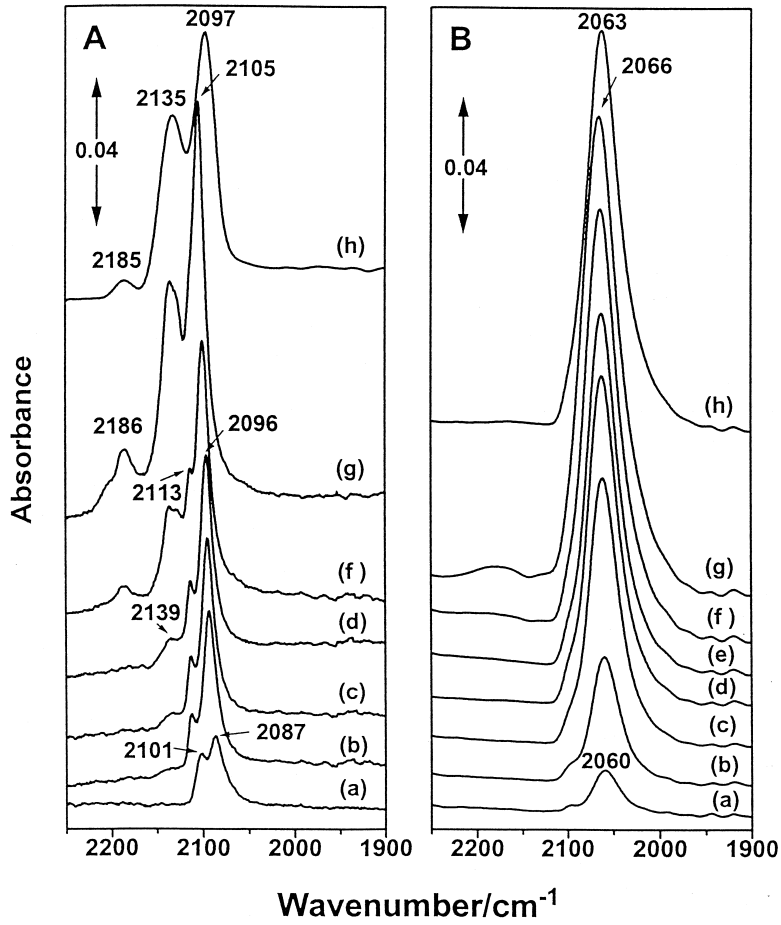

Fig. 5. Spectra as for Fig. 3 of (A) calcined/reduced/oxidised/reduced/oxychlorinated and (B) calcined/reduced/oxidised/reduced/oxychlorinated/reduced $Pt–Sn/Al_2O_3$.

same three bands as that after oxidation at 823 K. However, the band due to CO on Pt(II) was weaker and the band at 2122 cm^{-1} (Fig. 4), although not changed in intensity, was shifted to 2135 cm^{-1}. Thus, oxidised Pt sites were influenced by the presence of chlorine probably in PtO_xCl_y complexes spread over the alumina surface [28,29]. The band at 2105 cm^{-1} was 33% less intense than the corresponding band for oxidised catalyst suggesting a reduced dispersion of Pt°, in accordance with the XRD result which gave intense narrow peaks characteristic of large Pt° crystallites. A further factor which might have reduced the availability of Pt° sites for CO adsorption and caused the small upwards band shift of 5 cm^{-1} would be the existence of not only O-adatoms [24] but also Cl-adatoms in particle surfaces. Further evidence of an electronic effect of Cl atoms is provided by an additional band at 2101 cm^{-1} shifting to 2113 cm^{-1} at high coverage, not present for oxidised catalyst in the absence of chlorine. In some experiments, although not that leading to Fig. 5A (h), a clear maximum at 2114 cm^{-1} remained in the spectra after CO adsorption followed by evacuation.

Reduction of oxychlorinated catalyst gave spectra with a single strong band varying from 2060 to 2066 cm^{-1} with increasing coverage (Fig. 5B). This may be ascribed to adsorption at

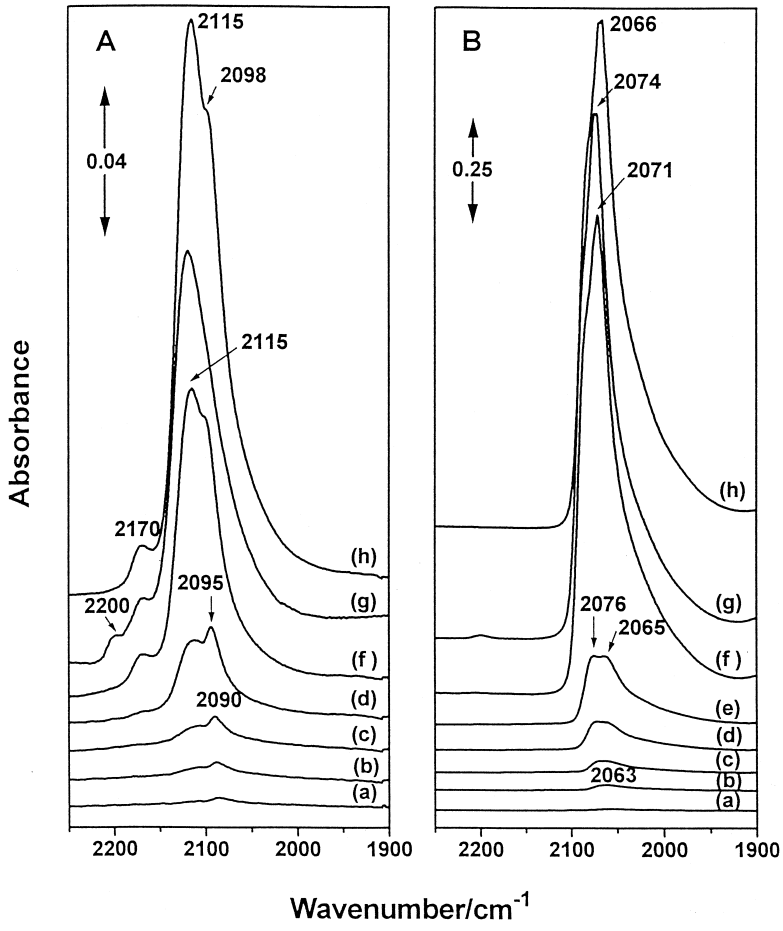

Fig. 6. Spectra as for Fig. 3 of (A) calcined and (B) calcined/reduced Pt/Al_2O_3.

isolated Pt° sites surrounded by Sn atoms in the surface of Pt–Sn alloy particles. There was no shoulder at 2077 cm^{-1} due to extended arrays of Pt atoms. The ν_{CO} band intensity was ca. 58% weaker than that for oxidised/reduced catalyst in accordance with the much reduced CO uptake for the alloy catalyst (Fig. 2). Identical reductions in maximum absorbance and CO/Pt would not be expected because of extinction coefficient variations for the infrared bands.

Spectra of calcined/reduced/oxychlorinated Pt–Sn/Al_2O_3 exposed to CO contained bands at (after evacuation) 2132, 2114 and 2098 cm^{-1} as in Fig. 5A but did not exhibit the band at 2185 cm^{-1}. Thus despite the similarity between the results in Figs. 3B and 4B, subsequent oxychlorination gave different results with respect to Pt(II) species for catalyst either subjected or not subjected to a previous oxidation (823 K)/reduction cycle. The different behaviour probably involved Pt dispersed on the alumina surface rather than in Pt° particles or in aggregates of PtO_2.

3.3. CO adsorption on Pt/Al_2O_3

Infrared spectra of CO on oxide-supported Pt catalysts show variations which depend on the support, metal loading and pretreatment conditions. Judgements concerning the effects of tin in the present catalysts therefore required data for Pt/Al_2O_3 at the same metal loading (3 wt.%) and after identical treatment sequences as

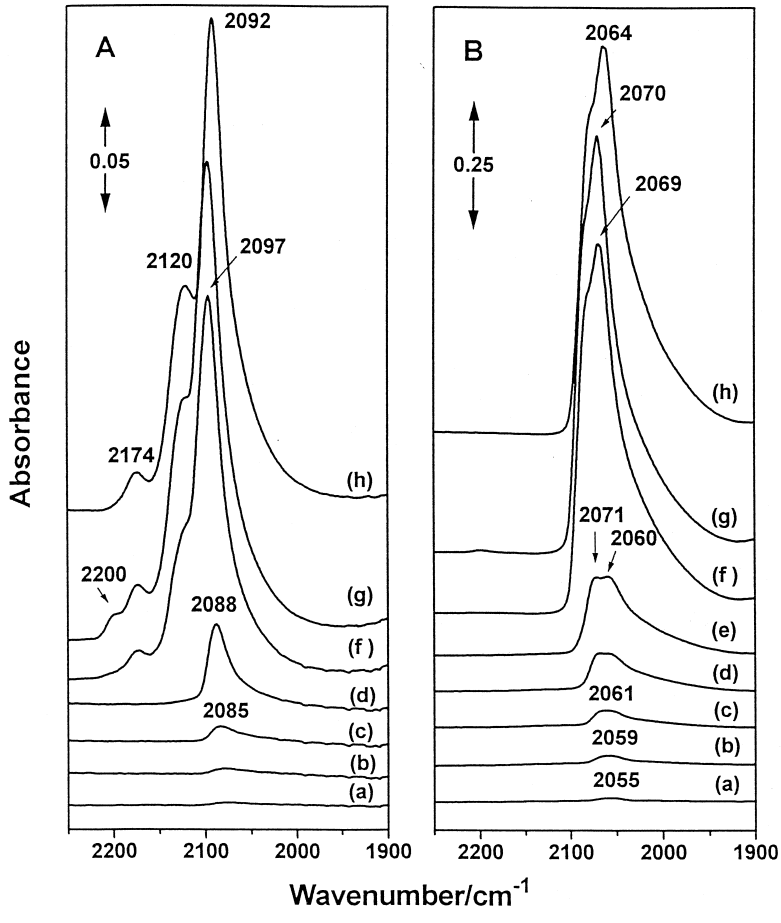

Fig. 7. Spectra as for Fig. 3 of (A) cacined/reduced/oxidised and (B) calcined/reduced/oxidised/reduced Pt/Al_2O_3.

those used in the study of $Pt–Sn/Al_2O_3$. The resulting spectra are in Figs. 6–8.

The chemisorption of CO on Pt/Al_2O_3 gave CO/Pt ratios of 0.56 for calcined/reduced catalyst, 0.36 for subsequently oxidised/reduced catalyst and 0.24 for subsequently oxychlorinated/reduced catalyst. The availability of Pt sites was much greater in the absence of Sn (Fig. 2), suggesting for Pt–Sn that exposed surfaces contained significant amounts of tin even when the bulk of the particles consisted predominantly of Pt (Fig. 1b and d). In accordance with results for 0.3% Pt/Al_2O_3 [14,15] high temperature oxidation followed by reduction decreased the Pt dispersion. However, the decrease in dispersion for 3% Pt after oxychlorination/reduction was unexpected compared with an earlier result for 0.3% Pt [15]. The different behaviour could be a result of either the different Pt loading or use of a different chlorinating agent. Comparing Pt–Sn and Pt showed that the addition of Sn gave the greatest proportional reduction in dispersion after oxychlorination/reduction rather than calcination/reduction or oxidation/reduction suggesting that it was the alloy particles (Fig. 1f) which contained the highest proportion of tin in their surfaces.

In broad terms, the infrared data agreed with the chemisorption results in that the intensities of the infrared bands due to Pt°–CO for reduced catalysts showed the same trends as the CO/Pt

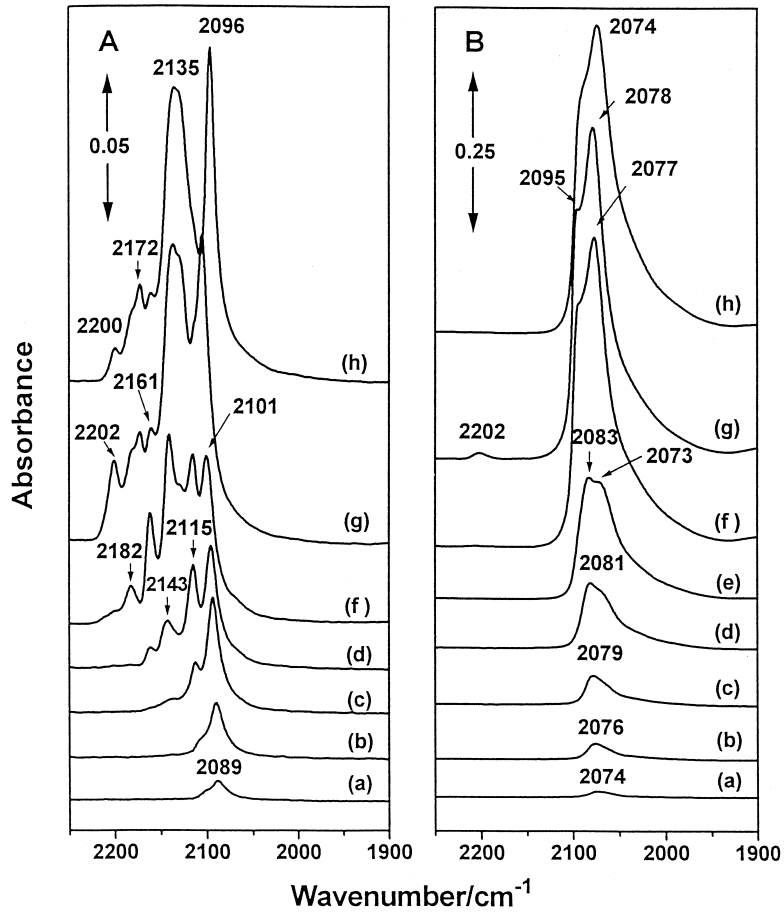

Fig. 8. Spectra as for Fig. 3 of (A) calcined/reduced/oxidised/reduced/oxychlorinated and (B) calcined/reduced/oxidised/reduced/oxychlorinated/reduced Pt/Al_2O_3.

values. In particular the biggest intensity decrease on adding Sn was for catalyst which had been oxychlorinated before reduction (Figs. 5B and 8B). However, the intensity decreases did not occur for CO adsorbed on calcined, oxidised or oxychlorinated catalysts (Figs. 3–8). Thus the effects of Sn on CO adsorption were only significant after reduction. In conjunction with the XRD results this suggests that segregation of Sn (as SnO_2 or tin oxide species on alumina) and Pt (as Pt°, PtO_2, chloro-Pt or oxychloro-Pt species on alumina or Pt) occurred during calcination, oxidation or oxychlorination, but that heat treatment in hydrogen promoted at least partial aggregation of Pt and Sn to form either alloy particles (during oxychlorination) or Pt° particles with surfaces having a high coverage by Sn atoms.

Spectra of CO on calcined Pt/Al_2O_3 (Fig. 6A) were similar to those for Pt–Sn (Fig. 3A) except for an additional band at ca. 2095 cm^{-1} due to linear adsorption on Pt° sites. Heating catalyst precursor in air at 673 K generated more Pt° sites for Pt alone than for Pt–Sn suggesting that Sn had hindered the partial decomposition of platinum oxide to Pt. Subsequent reduction of calcined Pt/Al_2O_3 and admission of CO gave a band at 2076 cm^{-1} supporting the conclusion that an identical band for $Pt–Sn/Al_2O_3$ may be ascribed to exposed arrays of Pt° atoms which were not influenced by tin. However, the dominant infrared band for CO on Pt was, for all coverages, at ca. 11–15 cm^{-1} higher wavenumber than the corresponding band for Pt–Sn, and was also much more intense in accordance with the CO/Pt results. These data are inexplicable in terms of Pt surfaces containing no tin in Pt–Sn catalyst, since a worse Pt dispersion induced by tin would imply bigger particles with fewer low coordination high energy sites and therefore, a blue shift rather than a red shift for the Pt°–CO band [26]. The red shift in band positions and the band intensity loss on adding Sn may be attributed to a decrease in the concentration of exposed Pt atoms in Pt° particle surfaces caused by surface Sn which reduced dipolar coupling interactions [27] between adsorbed CO molecules.

Spectra of CO on oxidised Pt/Al_2O_3 (Fig. 7A) showed, as for $Pt–Sn/Al_2O_3$ (Fig. 4A), that heat treatment of reduced catalyst in air at 823 K generated not only PtO_2 (2120 cm^{-1} [20]) but also O-covered [24] Pt° particles (2085–2097 cm^{-1}). Subsequent reduction gave spectra (Fig. 7B) which were similar to those for calcined/reduced catalyst. The dominant infrared band due to adsorbed CO was again blue-shifted from the result for $Pt–Sn/Al_2O_3$ (Fig. 4B) in accordance with the increased number of dipolar coupling interactions [27] experienced by each adsorbed CO molecule in the absence of surface tin.

Bands at 2182, 2135, 2115 and 2105 cm^{-1} (Fig. 8A) for CO on oxychlorinated Pt/Al_2O_3 resembled corresponding bands for $Pt–Sn/Al_2O_3$ (Fig. 4A) suggesting that the relevant Pt sites were not influenced by Sn, and also proving that none of these bands were due to CO interactions with tin. In particular, the identity of the band at 2105 cm^{-1} confirms the XRD result (Fig. 1e) showing that Pt in $Pt–Sn/Al_2O_3$ had segregated into Pt° particles, on which Pt sites were influenced by O-adatoms [24] and probably also surface Cl-adatoms. The band at 2135 cm^{-1}, attributed to CO interacting with PtO_xCl_y on the alumina support, was more intense relative to the other bands in the spectrum for Pt than for Pt–Sn catalysts. The spreading of Pt oxychloro-complexes over alumina during oxychlorination [28,29] was apparently partially impeded by competitive spreading of oxidic Sn species on the alumina surface [1,4,6–9]. Improved Pt dispersion after oxychlorination/reduction is recognised as resulting from enhanced spreading of Pt complexes during oxychlorination [15], and therefore inhibition of spreading induced by Sn at high loading probably contributed to the much lower CO/Pt uptakes for Pt–Sn than for Pt catalysts. Bands at 2200 (overlapping the vw band due to CO ligated to Al^{3+}), 2172 and 2161 cm^{-1} (Fig. 8A) for oxychlorinated Pt alone were not present for

Pt–Sn and are ascribed to CO ligated to surface Pt chloro (2200 and 2161 cm^{-1}) and Pt oxychloro species (2172 cm^{-1}) on alumina.

CO on reduced Pt/Al_2O_3 after oxychlorination gave two bands due to Pt°–CO (Fig. 8B) which were blue-shifted from the band positions for oxidised/reduced catalyst. These shifts are consistent with larger Pt particles [26] when oxychlorination rather than oxidation preceded reduction in accordance with the CO/Pt uptake data. This result contrasts with that for a 0.3% Pt/Al_2O_3 catalyst [14] where oxychlorination promoted dispersion. It appears that a high Pt loading (3%) either decreases the effectiveness of processes during oxychlorination which are favourable for high dispersion, or promotes aggregation of Pt into bigger particles during reduction. The bands for Pt alone were blue-shifted compared with the corresponding bands for Pt–Sn after oxychlorination/reduction confirming the effect of Sn as a diluent of the surface concentration of Pt atoms on Pt–Sn alloy (Fig. 1f) particles.

3.4. Heptane / hydrogen reactions over Pt–Sn / Al_2O_3

Catalytic activity for heptane reforming was decreased after an oxidation/reduction cycle (Fig. 2) which was in accordance with expectation for a catalyst not containing chlorine [14,16]. After an oxychlorination/reduction cycle the catalyst was even less active, this effect being in parallel with the concomitant decrease in CO uptake. Activities decreased as a function of time-on-line by, for example, ca. 50% after 2.9 h for catalysts not containing chlorine, but remained steady for catalyst which had been

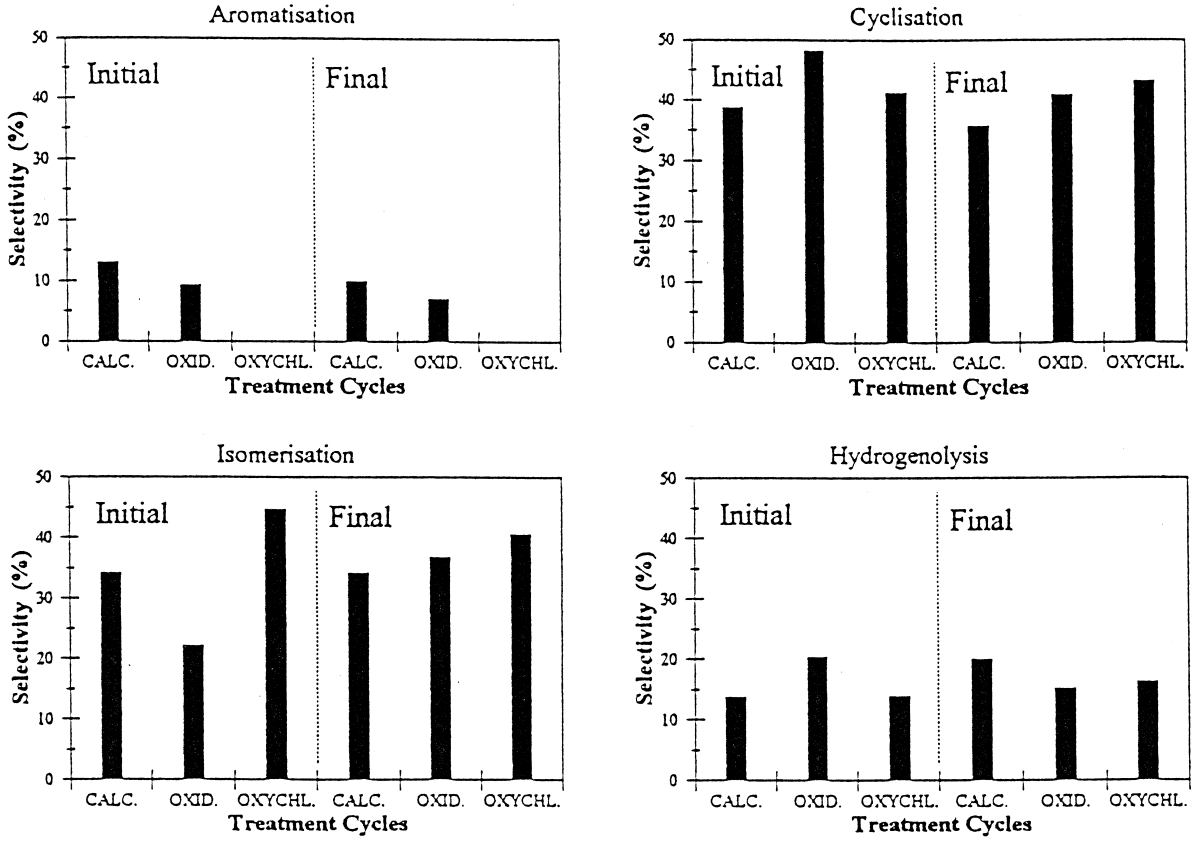

Fig. 9. Initial (0.08 h) and final (2.9 h) selectivities for heptane reaction over reduced Pt–Sn/Al_2O_3 after pretreatment by calcination (673 K), oxidation (823 K) or oxychlorination.

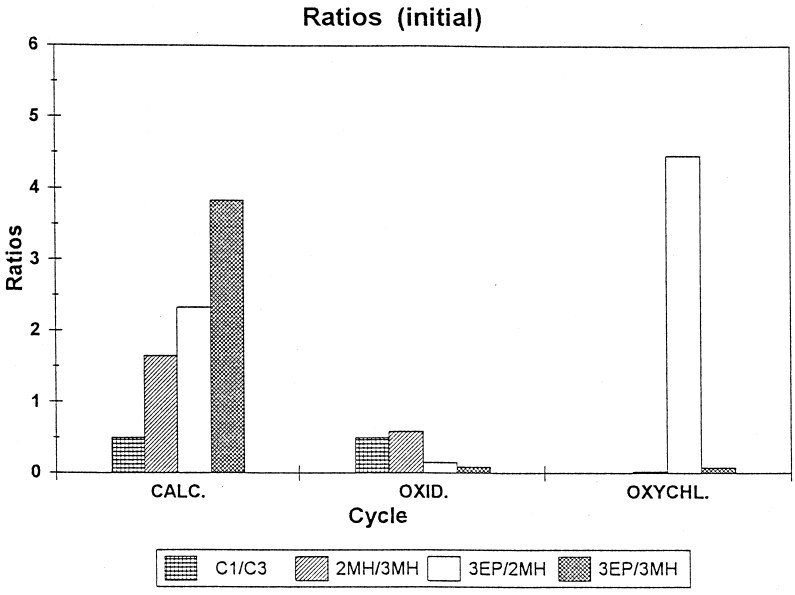

Fig. 10. Hydrogenolysis and isomerisation selectivities for reduced catalyst after calcination, oxidation and oxychlorination pretreatments.

oxychlorinated. Oxychlorination of a Pt–Sn/Al_2O_3 catalyst induced alloy formation on subsequent reduction and apparently hence hindered deactivation by coking. Selectivities for aromatisation, cyclisation, isomerisation and hydrogenolysis at 0.08 h and 2.9 h time-on-line are given in Fig. 9. Oxychlorinated catalyst was also the least sensitive to changing selectivities with time-on-line. For catalysts pretreated by calcination or oxidation, ethylcyclopentane was the dominant (75%) saturated cyclic product with some (25%) 1,2-dimethylcyclopentane and no saturated C_6 cyclics. However, for catalyst which had been oxychlorinated the only cyclic product was 1,2-dimethylcyclopentane even though the overall selectivity for cyclisation was maintained at ca. 40%. The initial selectivity for hydrogenolysis was slightly decreased after oxychlorination, although isomerisation was enhanced. The yields of all products were less after oxychlorination than after calcination or oxidation, the effect being greatest for aromatisation which did not occur for the oxychlorinated catalyst. Oxidised and calcined precursors gave Pt° particles with Sn on the surface but with exposed patches of Pt consisting of various sizes of Pt ensemble. Oxychlorinated precursor gave Pt–Sn alloy particles with surfaces containing isolated Sn-surrounded Pt atoms which were not able to catalyse cyclic C_6 formation and hence aromatisation to benzene or toluene.

Fig. 10 shows additional selectivity information. The C1/C3 ratio resulting from hydrogenolysis was the same for the two (calcined/reduced and oxidised/reduced) Cl-free Pt–Sn catalysts but, in contrast, no methane was formed for catalyst consisting of Pt–Sn alloy. The isomerisation results for methylhexanes (MH) and 3-ethylpentane (EP) showed that high temperature pre-oxidation considerably promoted MH formation with respect to EP, and favoured 3MH rather than 2MH (3MH > 2MH $\gg$ 3EP). After oxychlorination the product selectivities were in the order 3MH $\gg$ 3EP $\gg$ 2MH.

4. Discussion

Davis [30] has summarised the dominant states of Pt and Sn in reduced Pt–Sn/Al_2O_3 catalysts as Pt(atomic), Pt clusters and Pt–Sn alloy for Pt, and Sn aluminate and Pt–Sn alloy for Sn. The relative proportions of these states

depends on a variety of factors [30]. The present discussion is specifically concerned with the effect of oxychlorination on catalyst character, and also with the role of Sn in influencing the behaviour of exposed Pt sites on Pt° or Pt–Sn particles.

4.1. Calcined and oxidised catalyst precursors

Hobson et al. [31] showed that a calcined (773 K) Pt–Sn/Al_2O_3 catalyst precursor prepared from chlorine-containing materials consisted of small clusters of PtO_2 bonded to the support surface through a SnO_2-like layer. Similar treatment of the present Cl-free precursor led to a small proportion of the SnO_2 being present as crystallites which were of sufficient size to give an XRD pattern with weak broad peaks. The majority of the SnO_2 must have been spread over the alumina. The presence of PtO_2-like species, together with some Pt(II), was confirmed by the IR spectra although no XRD pattern for PtO_2 was detected showing that oxidic Pt species were also well dispersed. The similarities between the IR band positions for adsorbed CO on calcined Pt/Al_2O_3 and calcined Pt–Sn/Al_2O_3 hint at segregation of Pt and Sn oxides on alumina. However, the hindering effect of Sn on the decomposition of oxidised Pt to Pt° under calcination conditions suggests at least some intimacy of Pt and Sn species. Higher temperature (823 K) oxidation shifted the Pt(II)–CO band to 2180 cm^{-1} for Pt–Sn compared with 2174 cm^{-1} for Pt alone suggesting the promotion of Pt(II) sites which were probably involved in Pt–O–Sn bonding [32]. The absence of any XRD evidence for SnO_2 points to enhanced spreading of Sn oxide over alumina thus providing an enhanced opportunity for interaction between oxidic Pt and Sn.

4.2. The effect of Sn on ν_{CO} for reduced catalysts

Comparison of calcined, oxidised or oxychlorinated Pt and Pt–Sn catalysts after subsequent reduction showed that the effect of adding Sn to the catalyst was always to shift the dominant IR band due to Pt°–CO to lower wavenumbers. The question arises as to what extent these shifts were due to geometric [27,33] or electronic [1,25,34–38] effects or a mixture of both.

Previous IR studies of CO adsorption on Pt–Sn catalysts have shown that reductions in dipolar coupling provide the dominant effect of Sn addition on ν_{CO} band positions [27,33], although the extent of any contribution due to electronic effects may be a function of metal loading [35]. Catalyst prepared from highly dispersed Pt/Al_2O_3 by impregnation with tetrabutyl tin was described as Pt/SnO_x/Al_2O_3 and gave a band shift on adding Sn of $+6$ cm^{-1} attributed to a decrease in electron density of Pt atoms [35]. However, higher Pt loadings more equitable to that here gave catalyst described as Pt°Sn + SnO_x/Al_2O_3 for which no band shift attributable to an electronic effect was detected [35]. Burch [1] concluded that addition of Sn could make Pt either electron deficient via interaction with Sn(II) ions on alumina, or electron rich via formation of a solid solution of Sn in Pt. The latter is consistent with the view that Pt in Pt–Sn alloy is less electron deficient than in Pt alone [34,38], and would require that the electronic effect of adding Sn should contribute a negative (red) shift of ν_{CO}.

Infrared band intensities for CO at saturation coverages on reduced Pt/Al_2O_3 following calcination, oxidation or oxychlorination pretreatment showed a close parallel ($\pm 5\%$) with the corresponding CO uptakes. Blue shifts in band position with increasing coverage may primarily be attributed to enhanced dipolar coupling effects [27]. However, the shift in the band envelope maximum with coverage was much less pronounced for the oxychlorinated catalyst (Fig. 8B), and was much less than shifts for CO on single crystal surfaces [24]. Furthermore the band-envelope maxima were in general, particularly for pre-calcined and pre-oxidised catalysts, lower than those for single crystals suggesting that the bands should be assigned to CO at low

coordination, high energy Pt sites [24]. The blue shift in the dominant spectral maxima with increasing coverage could then also partially result from heterogeneity of Pt sites in reduced catalyst [26], higher energy sites being occupied first.

The decrease in CO uptake by Pt/Al_2O_3 after oxychlorination pretreatment followed by reduction could be ascribed to catalyst sintering, which may have occurred during the oxychlorination rather the subsequent reduction step [39]. However, this is difficult to rationalise in relation to the very small shift with coverage in the dominant band maximum due to adsorbed CO (Fig. 8B) because a sintered catalyst would exhibit similar [26] ν_{CO} shifts with increasing CO coverage due to dipolar coupling effects. Furthermore, oxychlorination can also improve Pt dispersion after reduction [15]. The very small band shift with coverage ($+4$ cm^{-1}) at the overall band maximum for the oxychlorinated catalyst suggests that Pt adsorption sites had become isolated in some way. One mechanism would involve slightly electron deficient isolated Pt atoms or small clusters (ca. 2–4 atoms) directly interacting with the alumina surface. This would also account for the blue shift of the infrared band (compared with calcined/reduced or oxidised/reduced Pt/Al_2O_3) at low coverages. However, this would constitute an improved dispersion of Pt which should be reflected in an increase rather than the observed decrease in CO uptake. This discrepancy can be resolved if the dominant IR band in Fig. 8 was due to the well-dispersed Pt interacting with alumina, whereas the weaker shoulder at 2095 cm^{-1} was due to CO on planar arrays of Pt atoms in the surface of large Pt particles containing the majority of the total Pt in the catalyst. The shoulder was at a higher wavenumber for the oxychlorinated catalyst than for calcined or oxidised catalysts which would be consistent with sintering to particles [26] with enhanced arrays of exposed Pt atoms akin to low-index crystal surfaces [24]. The spectral changes with coverage (Fig. 8B) suggest that the bands due to CO on the two types of site were coincident (2074 cm^{-1}) at low coverage, but with increasing coverage the band due to isolated or small-cluster-Pt on alumina was hardly shifted, whereas the band due to CO on large particles shifted significantly to ca. 2095 cm^{-1} in accordance with expectation [27] for dipolar coupling effects. Previous studies of 0.3% Pt/Al_2O_3 found that CO on oxidised/reduced [14] and oxychlorinated/reduced [15] catalyst gave a single band at 2074 cm^{-1} in accordance with this band corresponding to better dispersed Pt.

A contributing factor to the IR data for Pt in the absence of Sn might also be that the surface of the well-dispersed Pt species after oxychlorination/reduction contained atomic chlorine. A site blocking effect would reduce CO uptake, surface dilution of exposed Pt atoms by Cl would decrease dipolar coupling effects as a function of coverage, and the concomitant negative (red) shift in ν_{CO} due to the geometric effect would be more than compensated by a strong electron withdrawing effect of Cl inducing less electron donation into CO antibonding orbitals and a stronger C–O bond. Thus the band at 2095 cm^{-1} for high CO coverages, for which there was an appreciable blue shift with increasing coverage, may be ascribed to adsorption on sintered Pt° particles [26] with no surface Cl. The band at 2078 cm^{-1} may be attributed to CO on single Pt atoms or very small arrays of Pt adjacent to the alumina surface and strongly influenced by the e-withdrawing effects of Cl-adatoms. During oxychlorination catalyst was exposed to excess chlorine in the molar Cl:Pt ratio 133:1, which is equivalent to a total number of Cl atoms of 103 nm^{-2} of the support surface, more than enough to saturate available sites for Cl on alumina. Chlorine atoms have been proposed to exist on Pt particles after chlorination in the absence of oxygen [39]. Here it has been concluded that Cl probably exists together with O-adatoms on Pt° particles after oxychlorination. In accordance with the present suggestion Pt–Cl bonding has been detected in Pt–Sn catalysts containing chlorine, and also

the amount of Cl in surface layers on alumina in reduced catalyst is less than that in oxidised catalyst this effect being reversible during repeated oxidation/reduction cycles [40].

4.3. Reduced Cl-free Pt–Sn/Al_2O_3

The interaction of Pt in reduced Pt–Sn/Al_2O_3 with an Sn(II) oxidic layer dispersed over alumina [31,32] should decrease the Pt electron density [1] giving a blue shift in ν_{CO} [35], in contradiction to the present red shifts on adding Sn to Cl-free Pt catalyst. The observations that Pt–Sn/Al_2O_3 with similar Pt loading to that here and lower Sn loadings than here forms an alloy-type Pt–Sn° phase and that the addition of Sn induces no significant shift in ν_{CO} [35] is also at variance with the present results for Cl-free systems. The present red shift in the ν_{CO} band would be compatible with the existence of a close interaction between Pt°and Sn° leading to an enhanced e-density on Pt [1,34,38]. Such an interaction must primarily have been derived from deposited Sn on the surface of Pt° particles, although this does not exclude the possibility of a contribution from Pt–Sn phases which were either amorphous [35] or too small to be detected by XRD. Surface Sn would also have a geometric dilution effect on the concentration of surface Pt atoms and therefore would give a red shift in ν_{CO} due to a reduced number of dipolar coupling interactions experienced by each Pt-carbonyl [27]. The geometric effect is probably much more important than the electronic effect [27,33]. Thus, in accordance with conclusions of de Ménorval et al. [26] for Cl-free Pt–Sn/Al_2O_3, Sn° apparently partially covered high energy low coordination sites responsible for the dominant maxima in the IR spectra. The higher wavenumber shoulder associated with less well dispersed Pt° particles was also much reduced in intensity by the addition of Sn pointing either to considerable particle sintering or a high surface concentration of Sn°. In support of the latter was the smaller shift in the position of the shoulder with increasing coverage for Pt–Sn catalyst than for Pt alone. Thus the layer of Sn provided a geometric effect reducing dipolar coupling effects. This contrasts with a conclusion that an electronic and not a geometric effect was responsible for the influence of Sn on the catalytic properties of Pt(0.3%)–Sn/Al_2O_3 catalysts in which alloys were not formed [1]. Furthermore, the XRD results have shown that IR band shifts and reductions in CO uptake are not necessarily due to alloy formation [27], but may result from Sn deposited on the surface of Pt° particles [26,33,41,42]. The vast majority of cases in the literature for which alloy formation has been *proved* involve catalysts which contain Cl at some stage of the preparation, although a bimetallic alloy-type phase has been reported for Cl-free Pt–Sn/Al_2O_3 [32,35]. The present results are, however, consistent with metal particles having a Sn-rich surface [35].

4.4. Oxychlorinated / reduced Pt–Sn / Al_2O_3

The single IR band which was only slightly shifted with increasing coverage for oxychlorinated/reduced catalyst may be attributed to CO linearly adsorbed at Pt sites in the surface of Pt–Sn alloy particles with an homogeneously distributed Pt–Sn alloy on the surface [13,34]. Sparks et al. [43] deduced that Pt is all converted to alloy when the Sn:Pt ratio approaches 3:1 to 5:1 for 1%Pt supported on alumina. Here, for a Sn:Pt ratio of 2.47:1, the XRD only detected Sn–Pt alloy, although this does not preclude the existence of very small [44] Pt aggregates which could not be detected. However, the IR spectra suggested that one type of dominant Pt site was present. The total Sn content here was close to the maximum Sn content studied before [43] and the excess Sn (above a 1:1 Sn:Pt ratio) was also high in the present work. High excess Sn content favours alloy formation in the presence of Cl and probably hinders spreading of Pt over alumina by competition for sites on the support. Whereas chlorine may favour improved dispersion of Pt over alumina in

Pt/Al_2O_3 [15], in the case of $Pt–Sn/Al_2O_3$ [8] chlorine facilitates alloy formation. The low CO uptake suggests the alloy catalyst was sintered, and probably also enriched with Sn on the particle surfaces [13,18,19,38,41,45–47]. The XRD results show, in accordance with a conclusion for Pt/Al_2O_3 [39], that sintering occurred during oxychlorination prior to the reduction step. Combined with earlier results for the effects of oxidation/reduction cycles on Pt/Al_2O_3 dispersion [14,15] or on alloy formation which is diminished by oxidation treatments [48], the present data suggest that the reported disruption of Pt–Sn alloys and the increase in unalloyed surface Pt resulting from oxidation/reduction cycles in the absence of additional chlorine [49] may probably be ascribed to progressive Cl loss from the catalysts.

Bacaud et al. [7] reported that Sn in alumina-supported Pt–Sn catalysts underwent almost complete oxidation to Sn(IV) in CCl_4 vapour at 473 K in the absence of oxygen. Here, after treatment with 1,2-dichloropropane in the presence of oxygen, at least some of the Sn was aggregated into tin(IV) oxide crystallites, although these disappeared on subsequent reduction because of spreading of Sn(II) species over alumina [7,8,30,31] and the incorporation of Sn° into Pt–Sn 1:1 alloy particles. After oxychlorination Pt was present as either large crystallites of Pt° in particles covered with O-adatoms and possibly partially Cl-adatoms or as oxychloro-Pt and chloro-Pt complexes [8]. The complexes may exist on the surfaces of either Pt° particles or the alumina support [15,39].

The present results are consistent with conclusions that the dominant Pt–Sn alloy phase formed in Pt–Sn catalysts contains a 1:1 Pt:Sn ratio [5,12,13,17,40,41,43,44,48,50,51]. There was no evidence for either Pt_3Sn [5,48,50], $PtSn_2$ [13,50] or $PtSn_4$ [50]. The results here for catalyst with a Pt:Sn ratio of 1:2.47 also conform with analyses of PtSn:Pt ratios [17,43,50] and fractions of Sn in various Pt–Sn alloys [50] as a function of the stoichiometric Pt:Sn ratio. Srinivasan et al. [50] identified a range of Pt:Sn ratios for which Pt existed as Pt and PtSn, and at the lower end of Pt/Sn within that range the 1:1 PtSn alloy dominated over Pt. The present results, however, emphasise that these analyses are probably only valid for Cl-containing catalysts as in the absence of Cl, as before [8], no alloy was formed.

4.5. Heptane reforming reactions

Huang et al. [44] observed that particle aggregation and alloy formation occurred during the reforming of octane over $Pt–Sn/Al_2O_3$ catalysts prepared from Cl-containing precursors. The absence of evidence for similar effects here under conditions of lower temperature and pressure, particularly with regard to alloy formation, will have arisen because the absence of chlorine in reduced catalyst after oxidation/reduction meant that alloy formation was not facilitated, whereas for the oxychlorinated/reduced catalyst alloy formation was already largely complete before catalysis was carried out.

The activity of Pt/Al_2O_3 for reforming reactions is decreased by the addition of tin [7,38,43,52], and this has been attributed to alloy formation. Bacaud et al. [7] concluded that reaction over nonalloyed Pt was also inhibited. Catalyst sintering induced by higher temperature oxidation pretreatment of Pt/Al_2O_3 catalyst [14] leads to activity loss [16] which was ascribed to enhanced coking over larger Pt particles. Coking and the addition of Sn may have similar effects on reforming reactions as a result of the dilution of surface Pt [10]. However, the IR results suggest that for the present $Pt–Sn/Al_2O_3$ catalysts the dominant effect was the dispersion of Sn° over the surfaces of Pt° particles. Coq et al. [53] ascribed the catalytic effects of adding Sn to Pt/Al_2O_3 primarily to the dilution of the Pt surface by Sn, and Paál et al. [52] attributed activity and selectivity changes in similar systems to geometric ensemble effects involving Sn on metal particle surfaces. The effects here were magnified for Cl-containing

catalyst for which PtSn alloy formation was dominant, therefore providing far fewer exposed Pt atoms in Pt ensembles.

The addition of Sn to Pt/Al_2O_3 induces stability of both activity and selectivity [10,13,37]. Here the stabilising effect was only observed for Cl-containing catalyst implying that reaction-inhibiting coking [49] occurred on Pt ensembles on Pt° particles in Cl-free catalyst, but did not occur on the surface of PtSn alloy. Thus the favourable effects of Cl and Sn on stability are mutual and rely on the formation of alloy as the major catalytically active ingredient. Llorca et al. [13] similarly concluded that the presence specifically of PtSn alloy decreased catalyst deactivation.

Hydrogenolysis is decreased when Sn is added to Pt/Al_2O_3 because the geometric ensemble effect generates isolated exposed Pt atoms which are inactive for hydrogenolysis reactions [10,52,54,55]. Simultaneously isomerisation and C_5-cyclisation reactions are favoured [52,53,55], but aromatisation reactions may be favoured [10,37] or are disfavoured [55] particularly at high Sn content [10,40]. The present comparisons of initial selectivities for aromatisation, hydrogenolysis and isomerisation reactions for oxidised/reduced and oxychlorinated/reduced high Sn-content catalysts broadly concur with these effects showing that alloy formation enhanced the geometric effect of Sn on particle surfaces. Furthermore, increasing time-on-line for oxidised/reduced catalyst produced similar changes confirming that coking was also reducing Pt ensemble size [10]. However, the effects of alloying for hydrogenolysis in particular were fairly small supporting the contention that Pt° particles in Cl-free catalysts were partially covered in Sn which therefore provided a significant ensemble effect even in the absence of alloy.

Unexpectedly [52,55], the overall initial cyclisation selectivity was decreased by either Pt–Sn alloying after oxychlorination or by coking of Cl-free catalyst after oxidation pretreatment. Alloying clearly favoured 1,2-dimethylcyclopentane (as the only cyclisation product) rather than ethylcyclopentane which was also formed for the catalysts containing Pt° particles with surface Sn°. The geometric arrangement of exposed Pt atoms in the alloy surface apparently promoted 2,6-cyclisation rather than 1,5-cyclisation of heptane, although there may also have been an electronic effect of Sn on Pt [37,56]. Alloy formation also considerably disfavoured 2-methylhexane formation relative to 3-methylhexane and 3-ethylpentane.

Another influence on selectivities over Sn-containing catalysts is the deactivation of acidic sites on alumina caused by the spreading of Sn^{2+} ions over the alumina surface [6,7,9,38, 40,43], which therefore hinders bifunctional mechanistic pathways [43]. This effect might be expected to be greater for Cl-free catalyst than for Cl-containing catalyst because in the latter a high proportion of the total Sn present will be incorporated as Sn° into the bulk PtSn particle phase. Furthermore, the enhancement in acidity induced by chlorine might be expected to enhance catalysis involving the alumina surface. Ethylcyclopentane may be formed on alumina by a carbenium ion mechanism which would be favoured by chlorination and a decrease of site blocking by Sn. This is the reverse of the inhibition of ethylcyclopentane formation induced by oxychlorination/reduction suggesting that the dominant mechanistic effects here involved the Pt rather than the alumina surface. A notable feature of the results for isomerisation, cyclisation and hydrogenolysis is that changes in the initial selectivities induced by raising the pre-oxidation temperature from 673 K to 823 K were reversed after oxychlorination. The dispersion of Sn over Pt surfaces caused by high temperature oxidation followed by reduction blocked low-coordination high index Pt sites and therefore selectivity for hydrogenolysis was increased and for isomerisation was decreased. Alloy formation, however, generated isolated exposed Pt atom sites surrounded by Sn and therefore promoted restoration of the characteristic behaviour of isolated Pt sites.

Acknowledgements

We thank the Consejo Nacional de Investigaciones Cientificas y Tecnologicas, Venezuela and the University of Zulia, Venezuela for financial support (G.J.A.), and the Royal Society (London) for a University Research Fellowship (J.A.A.).

References

[1] R. Burch, J. Catal. 71 (1981) 348.
[2] B.H. Davis, G.A. Westfall, J. Watkins, J.J. Pezzanite, J. Catal. 42 (1976) 247.
[3] K. Balakrishnan, J. Schwank, J. Catal. 132 (1991) 451.
[4] Y. Li, K.J. Klabunde, B.H. Davis, J. Catal. 128 (1991) 1.
[5] G. Meitzner, G.H. Via, F.W. Lytle, S.C. Fung, J.H. Sinfelt, J. Phys. Chem. 92 (1988) 2925.
[6] B.A. Sexton, A.E. Hughes, K. Foger, J. Catal. 88 (1984) 466.
[7] R. Bacaud, P. Bussiere, F. Figueras, J. Catal. 69 (1981) 399.
[8] H. Lieske, J. Völter, J. Catal. 90 (1984) 96.
[9] J. Shen, R.D. Cortright, Y. Chen, J.A. Dumesic, Catal. Lett. 26 (1994) 247.
[10] B. Coq, F. Figueras, J. Catal. 85 (1994) 197.
[11] F.M. Dautzenberg, J.N. Helle, P. Biloen, W.M.H. Sachtler, J. Catal. 63 (1980) 119.
[12] J. Llorca, P. Ramírez de la Piscina, J.-L.G. Fierro, J. Sales, N. Homs, J. Catal. 156 (1995) 139.
[13] J. Llorca, N. Homs, J.-L.G. Fierro, J. Sales, P. Ramírez de la Piscina, J. Catal. 166 (1997) 44.
[14] J.A. Anderson, M.G.V. Mordente, C.H. Rochester, J. Chem Soc., Faraday Trans. 1 (85) (1989) 2983.
[15] M.G.V. Mordente, C.H. Rochester, J. Chem. Soc., Faraday Trans. 1 (85) (1989) 3495.
[16] J.A. Anderson, M.G.V. Mordente, C.H. Rochester, J. Chem. Soc., Faraday Trans. 1 (85) (1989) 2991.
[17] R. Srinivasan, B.H. Davis, Appl. Catal. A 87 (1992) 45.
[18] R. Bouwman, P. Biloen, J. Catal. 48 (1977) 209.
[19] S. de Miguel, A. Castro, O. Scelza, J.L.G. Fierro, J. Soria, Catal. Lett. 36 (1996) 201.
[20] Y. Barshad, X. Zhou, E. Gulari, J. Catal. 94 (1984) 128.
[21] Y.A. Lokhov, A.A. Davidov, Kinet. Katal. 21 (1980) 1523.
[22] L.H. Little, C.H. Amberg, Can. J. Chem. 40 (1962) 1997.
[23] R. Barth, R. Pitchai, R.L. Anderson, X.E. Verykios, J. Catal. 116 (1989) 61.
[24] C. De La Cruz, N. Sheppard, Spectrochim. Acta A 50 (1994) 271.
[25] N. Sheppard, T.T. Nguyen, Adv. Infrared Raman Spectrosc. 5 (1978) 67.
[26] L.C. de Ménorval, A. Chaqroune, B. Coq, F. Figueras, J. Chem. Soc., Faraday Trans. 93 (1997) 3715.
[27] A.G.T.M. Bastein, F.J.C.M. Toolenaar, V. Ponec, J. Catal. 90 (1984) 88.
[28] H. Lieske, G. Lietz, H. Spindler, J. Völter, J. Catal. 81 (1983) 8.
[29] T.J. Lee, Y.G. Kim, J. Catal. 90 (1984) 279.
[30] B.H. Davis, in: M.E. Davis, S. Suib (Eds.), Selectivity in Catalysis, ACS Symposium Series, Am Chem. Soc., Washington, DC, 517, 1993, p. 109.
[31] M.C. Hobson, S.L. Goresh, G.P. Khare, J. Catal. 142 (1993) 641.
[32] A. Caballero, H. Dexpert, B. Didillon, F. LePeltier, O. Clause, J. Lynch, J. Phys. Chem. 97 (1997) 11283.
[33] J. Schwank, K. Balakrishnan, A. Sachdev, in: L. Guczi, F. Solymosi, P. Tétényi (Eds.), New Frontiers in Catalysis, Proc. 10th Int. Congr. Catal., Elsevier, Budapest, 1993, p. 905.
[34] B. Shi, B.H. Davis, J. Catal. 157 (1995) 626.
[35] E. Merlen, P. Beccat, J.C. Bertolini, P. Delichere, N. Zanier, B. Didillon, J. Catal. 159 (1996) 178.
[36] K. Balakrishnan, J. Schwank, J. Catal. 138 (1992) 491.
[37] R. Burch, L.C. Garla, J. Catal. 71 (1981) 360.
[38] R. Srinivasan, B.H. Davis, J. Mol. Catal. 88 (1994) 343.
[39] A. Melchor, E. Garbowski, M.-V. Mathieu, M. Primet, J. Chem. Soc., Faraday Trans. 82 (1986) 3667.
[40] B.H. Davis, in: L. Guczi, F. Solymosi, P. Tétényi (Eds.), New Frontiers in Catalysis, Proc. 10th Int. Congr. Catal., Elsevier, Budapest, 1993, p. 889.
[41] J.W. Curley, O.E. Finlayson, in: T.J. Dines, C.H. Rochester, J. Thomson (Eds.), Catalysis and Surface Characterisation, Royal Society of Chemistry, Cambridge, 1992, p. 276.
[42] K. Balakrishnan, J. Schwank, J. Catal. 127 (1991) 287.
[43] D.E. Sparks, R. Srinivasan, B.H. Davis, J. Mol. Catal. 88 (1994) 359.
[44] Z. Huang, J.R. Fryer, C. Park, D. Stirling, G. Webb, J. Catal. 159 (1996) 340.
[45] H. Verbeek, W.M.H. Sachtler, J. Catal. 42 (1976) 257.
[46] Y. Weishen, L. Liwu, F. Yining, Z. Jingling, Catal. Lett. 12 (1992) 267.
[47] R. Bouwman, P. Biloen, Anal. Chem. 46 (1974) 136.
[48] A. El Abed, S. El Qebbaj, M. Guerin, C. Kappenstein, M. Saouabe, P. Marecot, J. Chim. Phys. 92 (1995) 1307.
[49] S.M. Stagg, C.A. Querini, W.E. Alvarez, D.E. Resasco, J. Catal. 168 (1997) 75.
[50] R. Srinivasan, R. Sharma, S. Su, B.H. Davis, Catal. Today 21 (1994) 83.
[51] Y.-X. Li, K.L. Klabunde, B.H. Davis, J. Catal. 128 (1991) 1.
[52] Z. Paál, A. Györy, I. Uszkurat, S. Olivier, M. Guérin, C. Kappenstein, J. Catal. 168 (1997) 164.
[53] B. Coq, A. Chaqroune, F. Figueras, B. Ncira, Appl. Catal. A 82 (1992) 231.
[54] J. Völter, U. Kürschner, Appl. Catal. 8 (1983) 167.
[55] Y. Zhou, S.M. Davis, Surf. Sci. Catal. 482 (1992) 160, A.C.S. Symposium Series.
[56] M.T. Paffet, S.C. Gebhard, R.G. Windham, B.E. Koel, J. Phys. Chem. 94 (1990) 6831.